Macromolecules

Article

Cite This: Macromolecules 2018, 51, 3107−3115

Thermodynamic Interactions in a Model Polydiene/Polyolefin Blend Based on 1,2-Polybutadiene

Jialin Qiu,[†] Katrina I. Mongcopa,[†] Ruixuan Han,[†] Carlos R. López-Barrón,[‡] Megan L. Robertson,*[,†] and Ramanan Krishnamoorti*[,†]

[†]Department of Chemical and Biomolecular Engineering, University of Houston, Houston, Texas 77204, United States

[‡]ExxonMobil Chemical Company, Baytown, Texas 77520, United States

Supporting Information

ABSTRACT: Thermodynamic interactions in polydiene/polyolefin blends composed of 1,2-polybutadiene (1,2-PBD) and fully saturated (with deuterium) 1,2-PBD were explored with small-angle neutron scattering (SANS). Two methods were employed to extract the temperature dependence of the Flory−Huggins interaction parameter, χ, from SANS data obtained in the single-phase region. First, Zimm analysis was conducted employing data obtained at low scattering angles, providing a model-independent method of characterizing χ. Next, the random phase approximation was fit to the full angle-dependent absolute scattering intensity. The χ parameter for 1,2-PBD/saturated 1,2-PBD was found to be large in magnitude at low temperatures and exhibited a strong temperature dependence. The experimentally measured χ, at high temperatures, was in agreement with predictions of solubility parameter theory based on PVT properties of the individual components. The large and strongly temperature-dependent χ parameter of the 1,2-PBD/saturated 1,2-PBD mixture is an attractive feature enabling facile material processing and is in stark contrast to behavior observed in more traditionally studied polyolefin/polyolefin and polydiene/polydiene pairs.

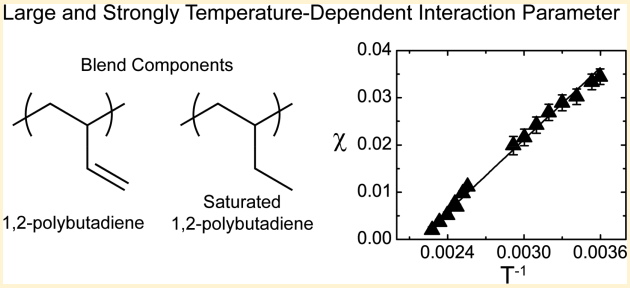

INTRODUCTION

Multicomponent polymer systems, such as polymer blends, block copolymers, and polymer/additive mixtures, exhibit properties that are highly dependent on interactions between the material components, typically described by the Flory−Huggins interaction parameter, χ. For example, χ governs the interfacial tension and interfacial width of an immiscible polymer blend,[1−3] which impact the blend mechanical properties.[4] Similarly, χ influences the interfacial width and equilibrium domain spacing of a block copolymer,[5] which are relevant for applications such as membranes and templates.[6] Additionally, accessing targeted equilibrium phases in polymer mixtures, whether it be a miscible polymer/additive mixture such as in the case of a plasticized polymer, immiscible rubber toughened polymer blend, or nanophase-separated block copolymer, depends on knowledge of the temperature dependence of the χ parameter.[7−9]

Polydienes and polyolefins are dominant materials employed in elastomer applications, such as sealants, rubber tires, adhesives, and impact modifiers, among others. Blends of polydienes generally exhibit small χ parameters with weak temperature dependencies,[10] such as in the case of polybutadiene mixtures,[11,12] and blends of polybutadienes with polyisoprenes.[13,14] Interactions in blends of polyolefins have been extensively studied,[10] and generally they also exhibit small and weakly temperature-dependent χ parameters, such as in the case of blends of saturated polybutadienes (with ∼10−20% differences in 1,2-polybutadiene content between blend components);[15−18] blends of saturated polybutadienes and saturated polyisoprenes;[18,19] polypropylene-based blends;[20−23] blends of various types of polyethylenes, or polyethylene mixed with saturated polyisoprene, poly(1-hexene), poly(1-butene), or poly(1-octene);[24−29] polyisobutylene-based blends;[30] and blends of olefin oligomers.[31] An important exception is the blend composed of saturated polybutadiene with 7% 1,2-addition and saturated polybutadiene with 90% 1,2-addition, which exhibited a χ parameter with a much stronger temperature dependence.[19] Additionally, blends of appropriately chosen polyolefins with polyisobutylene led to large negative χ parameters and lower critical solution temperature behavior.[32,33]

Interactions in mixtures of polydienes and polyolefins are less understood than polyolefin/polyolefin and polydiene/polydiene pairs. Two notable literature studies report the large and strongly temperature-dependent χ parameter in a blend of polyisoprene and saturated polyisoprene (both containing 93% 1,4-addition)[34] as well as that in a blend of polyisoprene (with 94% 1,4-addition) and saturated polybutadiene (with 99% 1,2-addition).[35] Blends of polybutadienes and their saturated analogues have not been explored.

Received: October 10, 2017
Revised: March 23, 2018
Published: April 10, 2018

DOI: 10.1021/acs.macromol.7b02181
Macromolecules 2018, 51, 3107−3115

We have chosen to employ a model system for exploring thermodynamic interactions in polydiene/polyolefin blends: a blend composed of 1,2-polybutadiene (1,2-PBD) and saturated 1,2-PBD. Polymerization of the 1,3-butadiene monomer produces copolymers containing both 1,4-polybutadiene (1,4-PBD) and 1,2-PBD repeat units; saturation of these copolymers with hydrogen or deuterium produces copolymers of polyethylene (i.e., saturation of the 1,4-PBD repeat units) and poly(ethylethylene) (i.e., saturation of the 1,2-PBD repeat units, also called poly(1-butene)). The 1,2-PBD/saturated 1,2-PBD blend has many attractive features as a model system. First, the blend components are amorphous polymers with glass transition temperatures below room temperature, allowing for an extended temperature range for characterization of χ. Second, model polybutadiene with high 1,2 content (>99%) can be synthesized through anionic polymerization in the presence of polar additives. The absence of copolymers containing both 1,2 and 1,4 repeat units simplifies interpretation of the thermodynamic data. Additionally, analysis of data is facilitated by the synthesis of low-dispersity polymers, also accessed using anionic polymerization. Finally, these blends are not anticipated to exhibit specific interactions such as hydrogen bonding.

Here, we present characterization of χ through analysis of small-angle neutron scattering (SANS) data obtained from single phase blends of 1,2-PBD and saturated 1,2-PBD at 50/50 compositions. Saturation of 1,2-PBD was conducted with deuterium, providing neutron contrast. The temperature dependence of χ was obtained through Zimm analysis and fitting of the random phase approximation to SANS data. The resulting χ parameter was compared to that obtained through predictions of solubility parameter theory based on PVT properties of the individual components.

EXPERIMENTAL DETAILS

Polymer Synthesis. *Anionic Polymerization of 1,3-Butadiene.* Polybutadiene (PBD) homopolymers with high 1,2 content were synthesized by anionic polymerization. The 1,3-butadiene (≥99%, Aldrich) monomer was condensed to a Schlenk flask containing calcium hydride (CaH_2, Sigma-Aldrich) in a dry ice/isopropanol (IPA) bath and degassed with several freeze−pump−thaw cycles. After stirring overnight at dry ice/IPA temperature, the monomer was further degassed and distilled to a second Schlenk flask containing *sec*-butyllithium (1.4 M in cyclohexane, Sigma-Aldrich) in dry ice/IPA (cyclohexane was removed from *sec*-butyllithium by distillation prior to use). After the distillation process, the flask containing monomer and *sec*-butyllithium was kept overnight at dry ice/IPA temperature with stirring. The monomer was further degassed through additional freeze−pump−thaw cycles, distilled to a second Schlenk flask containing *sec*-butyllithium (with cyclohexane removed) in dry ice/IPA, and kept overnight in dry ice/IPA temperature with stirring. The monomer was degassed again through additional freeze−pump−thaw cycles and distilled to a flame-dried graduated ampule in dry ice/IPA.

1,2-Dipiperidinoethane (DIPIP, 98%, Fischer Scientific) was distilled over CaH_2 (Sigma-Aldrich) prior to use and, in some cases, was also synthesized according to ref 36. Briefly, piperidine (54.0 g, 634 mmol) was placed in a two-neck flask equipped with a stir bar and connected to a reflux condenser. 1,2-Dibromoethane (29.8 g, 159 mmol) was then added dropwise into the flask via syringe while refluxing (95−100 °C). The reaction proceeded for 4 h, and a solid precipitate was formed. The mixture was then diluted with diethyl ether, and the ether wash was transferred into a clean round-bottom flask using a funnel and filter paper to filter out the solid. The filtrate was concentrated to give the crude product, which was further purified by distillation under vacuum to give a clear, light yellow liquid. The purified DIPIP was stored in a nitrogen glovebox (Vacuum Atmospheres).

Water and oxygen-free cyclohexane were transferred to a flame-dried Schenk flask from a Pure Process Technology solvent purification system. In the nitrogen glovebox, the initiator *sec*-butyllithium was transferred to the flask containing cyclohexane. DIPIP and cyclohexane were also transferred to a flame-dried ampule in the glovebox. Both the flask and ampule were tightly closed and removed from the glovebox.

A multineck reactor containing a pressure gauge and pressure relief valve was assembled. The reactor setup was placed under vacuum and then flushed with argon gas (argon pressure was slightly above ambient but always kept under 5 psi). This process was repeated multiple times. Under slight argon pressure (around 4−5 psi), the cyclohexane/initiator flask and cyclohexane/DIPIP ampule from the glovebox were attached to the reactor. Additionally, the flask containing purified 1,3-butadiene was connected to the reactor using a flexible metal tube, while maintaining the monomer at dry ice/IPA temperature. Vacuum−argon cycles were completed once again on the assembled reactor setup. At the end of the cycle, the reactor setup was kept under slight argon pressure (around 4−5 psi). The valve that connected the reactor to the Schlenk line was closed before charging the reactor. The reactor was cooled to 0 °C using an ice bath, and the valve was opened to allow cyclohexane/initiator to flow into the reactor with stirring. Next, the valve was opened to allow cyclohexane/DIPIP to flow into the reactor. Finally, the cold 1,3-butadiene flask was elevated, and the valve was opened to allow 1,3-butadiene to flow into the reactor. The reactor pressure was monitored to ensure it did not exceed 5 psi during this process. Following a suitable reaction time (varying from 3 to 12 h based on the target molecular weight), the reaction was terminated using degassed isopropanol. Butylated hydroxytoluene (BHT, ≥99%, Sigma-Aldrich) was added to the solution after 30 min of termination at a level of 0.05 g BHT per 1 g polymer. The polymer was recovered by precipitation in excess methanol/acetone (50/50). Because of the loss of BHT through precipitation, the same amount of BHT was added again to the precipitated polymer dissolved in cyclohexane. After removing the solvent through evaporation in a fume hood, the polymer was dried under vacuum at 40 °C for 2 weeks until residual solvent was not detected by NMR, and an analytical balance indicated no measurable mass change.

Saturation of Polybutadiene. PBD polymers were dissolved in cyclohexane (1 g polymer per 100 mL solvent) and purged with argon. The solution was transferred to a Parr high-pressure reactor along with palladium catalyst (5% on barium sulfate, unreduced, Strem Chemical). 1 g of catalyst was added per gram of polymer. The reactor was purged with argon gas and then allowed to equilibrate at 90 °C. 500 psi of deuterium was added to the reactor, and the reactor was allowed to stir for 2 days. At the end of the reaction, the reactor was cooled to room temperature, deuterium was released under an excess of nitrogen, and the polymer solution was recovered. The solution was filtered with a stack of four filters (in the order of 11, 8, 11, and 8 μm) in a metal filter assembly under slight nitrogen pressure (50 psi) to remove the catalyst. The saturation procedure was repeated until full saturation (<1% unsaturated content). The final solution was filtered using a 0.2 μm filter. After evaporating solvent in a fume hood, the polymer was dried in a vacuum oven at 40 °C for 2 weeks until residual solvent was not detected by NMR, and an analytical balance indicated no measurable mass change.

Polymer Characterization. *Gel Permeation Chromatography.* Weight-average molecular weight (M_w) and dispersity ($Đ$) were characterized through gel permeation chromatography (GPC) using a Malvern GPCMax instrument containing two Agilent ResiPore columns using THF (OmniSolv, HPLC grade) as the mobile phase at 30 °C. The flow rate was 1 mL/min, and the injection volume was 100 μL at a polymer concentration of 1−5 mg/mL. Triple detection (including light scattering) was employed for absolute molecular weight determination. The dn/dc values for 1,2-PBD and saturated 1,2-PBD were characterized as 0.105 ± 0.0002 and 0.067 ± 0.002, respectively.

Nuclear Magnetic Resonance. ^{1}H NMR experiments were performed on a JEOL ECA-400 instrument using deuterated chloroform (Cambridge Isotope Laboratories, Inc., 99.8% D) as the solvent. Chemical shifts were referenced to the solvent proton resonance (7.24 ppm).

DOI: 10.1021/acs.macromol.7b02181
Macromolecules 2018, 51, 3107−3115

Density Measurement. A home-built density gradient column was employed for measurement of polymer densities. Samples were prepared on glass slides and annealed at room temperature under vacuum overnight to remove bubbles. The density gradient was prepared in a graduated glass column using mixtures of methanol and ethylene glycol at low (0.82 g/mL) and high (0.98 g/mL) densities. Calibrated beads (American Density Materials) were added to the column to create a height−density calibration curve. The slide containing the polymer was cooled in liquid nitrogen to ensure the polymer was below its glass transition temperature, and a razor blade (also cooled in liquid nitrogen) was used to cut a small piece of polymer from the slide. The polymer was transferred to the column while remaining below the glass transition temperature. This process was repeated until multiple specimens were transferred to the column. The bead and polymer positions were monitored over multiple days (typically three) until they had equilibrated. The polymer density was then calculated from the calibration curve.

The number of deuterium atoms per repeat unit with empirical formula $(CH_2)_x$, n_D, was characterized through density measurements, employing eq 1:

$$n_D = \frac{M_{o,H}\left(\frac{\rho_{PBD\text{-}X\text{-}D}}{\rho_{PBD\text{-}X\text{-}H}} - 1\right)}{(m_d - m_h) + M_{o,H}\left(\frac{\rho_{PBD\text{-}X\text{-}D}}{\rho_{PBD\text{-}X\text{-}H}}\right)\left(\frac{\beta}{2x}\right)} \quad (1)$$

where x is the number of CH_2 groups in a polymer repeat unit, $\rho_{PBD\text{-}X\text{-}D}$ and $\rho_{PBD\text{-}X\text{-}H}$ are densities of deuterated and hydrogenated polymers obtained from the same parent polydiene, $M_{o,H}$ is the molecular weight of the hydrogenated polymer, m_d and m_h are the atomic weights of deuterium and hydrogen, and β is the fractional reduction in molar volume for the full replacement of hydrogen with deuterium (defined as $\beta = ((V_D)_{PD} - V_H)/V_H$, where $(V_D)_{PD}$ and V_H are the specific volumes of the perdeuterated and hydrogenated species, respectively). In our study, a repeat unit is defined such that $x = 4$, and β was taken to be 0.002, an average of that reported in the literature studies,[37−39] following ref 16.

Small-Angle Neutron Scattering. Blends of 1,2-polybutadiene (1,2-PBD) and saturated 1,2-PBD at 50/50 compositions (which was near the critical composition for Blend B) were prepared by codissolving the components in cyclohexane and stirring for several hours. The solvent was removed by evaporation in a fume hood, followed by drying to a constant weight in a vacuum oven at 40 °C (typically 1 week). The blends were loaded on top of a quartz window with an aluminum spacer, placed in the vacuum oven to remove bubbles, and then sandwiched with another quartz window. The outer area circumference of the quartz was sealed with Dow silicone adhesive (Dow Corning Number 736 High-Temperature Silicone), leaving a small opening at the top for thermal expansion of the polymer. The samples were secured in demountable brass cell holders. Two temperature control environments were used: a 7-position heating block with cartridge heaters (for Blend B) and a 10-position heating block with a circulating fluid (for blend A).

SANS measurements were obtained on the NG-7 and NGB 30m beamlines at the National Institute of Standards and Technology Center for Neutron Research. Measurements were performed with a neutron wavelength of 6 Å and three sample-to-detector distances of 13, 4 and 1 m, allowing access to a scattering wave-vector magnitude, $q = (4\pi/\lambda)\sin(\theta/2)$, ranging from 0.003 to 0.5 $Å^{-1}$.[40] Samples of thickness 1 mm were employed. The total scattering intensity was corrected for detector sensitivity, background, and empty cell contributions as well as sample transmission and thickness.[41] The incoherent background I_{inc} was quantified at each temperature as the slope determined from a plot of $I_{total}\,q^4$ vs q^4 at high q (i.e., in the range of 0.2−0.3 $Å^{-1}$; a representative plot is shown in Figure S1). In the case of blend B, coherent scattering from the pure deuterated component was also subtracted.[42]

RESULTS AND DISCUSSION

Synthesis and Characterization of 1,2-Polybutadiene (1,2-PBD) and Saturated 1,2-PBD. Polybutadiene with high 1,2 content and low dispersity ($Đ$) was synthesized through anionic polymerization of 1,3-butadiene employing Schlenk line techniques. The polymerization was conducted in cyclohexane at 0 °C, using *sec*-butyl lithium (sBuLi) as the initiator and 1,2-dipiperidinoethane (DIPIP) as a polar additive to modify the 1,2 content (Scheme 1).[43−46] DIPIP was synthesized through

Scheme 1. Synthesis of 1,2-Polybutadiene through Anionic Polymerization of 1,3-Butadiene

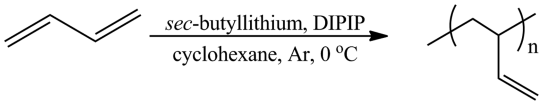

literature procedures[36] (NMR data shown in Figure S2). Two reaction parameters were optimized in early synthetic attempts. First, it was discovered that a very short reaction time was required to achieve full conversion, and stopping the reaction prior to full conversion helped avoid side reactions which increase the dispersity.[47] Second, the chosen DIPIP:sBuLi ratio governed the % 1,2 content of the polymer. We initially used a lower ratio (1:1 or 2:1) and found the % 1,2-addition was in the range of 95−97%. Increasing this ratio to 10:1 increased the % 1,2-content to 99% or greater. The polybutadienes were fully saturated with deuterium using a palladium catalyst (Scheme 2). Saturation reactions were repeated until high % saturation was achieved (>99%).

Scheme 2. Saturation of 1,2-Polybutadiene

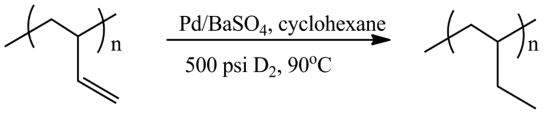

^{1}H NMR spectra showed characteristic peaks for 1,2-PBD and saturated 1,2-PBD (Figures S3 and S4). The polymers contained high 1,2 content (95% and above), and saturated polymers contained less than 1% of unsaturated repeat units. Characteristics of polymers employed in blends discussed in this article are shown in Table 1.

Characterization of the Flory−Huggins Interaction Parameter through Small-Angle Neutron Scattering (SANS). Binary blends containing 1,2-PBD and saturated 1,2-PBD were prepared using solvent casting techniques (at 50/50 compositions). Both blends were encapsulated between quartz disks with an aluminum spacer for small-angle neutron scattering (SANS) measurements, which were conducted at the NIST Center for Neutron Research. SANS data (coherent scattering intensity I_{coh} as a function of scattering vector q) are shown in Figure 1 (the total scattering intensity, I_{total}, as a function of q is shown in Figure S6). I_{coh} shows a systematic decrease in the low-q plateau as the temperature is increased. The data converge at high q as expected.

The SANS data were analyzed to extract the Flory−Huggins interaction parameter, χ, describing the interactions between the blend components, 1,2-PBD, and saturated 1,2-PBD. The scattering intensity at $q = 0$ is related to the change in the Gibbs free energy due to mixing, ΔG, of the polymer mixture:

$$S^{-1}(q = 0) = \frac{1}{k_B T}\frac{\partial^2 \Delta G}{\partial \phi_1^2} \quad (2)$$

DOI: 10.1021/acs.macromol.7b02181
Macromolecules 2018, 51, 3107−3115

Table 1. Polymer Characteristics

blend	polymer	M_w (kg/mol)[a]	$Đ$[a]	% 1,2 addition[b]	% saturation[b]	ρ (g/mL) at 23 °C[d]	N_{mon}[e]	N at 23 °C[f]	n_D[g]
A	PBD-2k	1.9	1.03	94.5 ± 0.9	NA	0.8766	35.5	36.3	NA
	PBD-3k-D	3.2[c]	1.06	97.4 ± 0.6	99.1 ± 0.6	0.9025	59.5	64.1	2.42
B	PBD-7k	6.8	1.03	99.0 ± 0.5	NA	0.8868	124.8	126.5	NA
	PBD-7k-D	6.8[c]	1.03	99.0 ± 0.5	99.2 ± 0.4	0.9040	124.8	134.4	2.42

[a]Measured through GPC using light scattering (Figure S5). [b]Measured through ^{1}H NMR (Figures S3 and S4). Error of analysis is reported. [c]Measured for the polydiene precursor to the deuterated polymers. [d]Measured using a density gradient column. Error in density is quantified as 0.0003 for all measurements. [e]Number of monomer repeat units (C_4H_6 or C_4H_8) per chain. [f]Number of repeat units per chain based on a reference volume of 100 Å^3. Temperature dependence of v_{mon} was accounted for using the thermal expansion coefficient of 0.000 68 K^{-1} reported in refs 48 and 49. [g]Number of deuterium atoms per C_4 repeat unit, calculated from density measurements on fully hydrogenated and deuterated 1,2-polybutadiene pairs (eq 1). Densities of fully hydrogenated polymers: PBD-4k-H (0.8643 ± 0.0003) and PBD-7k-H (0.8657 ± 0.0003).

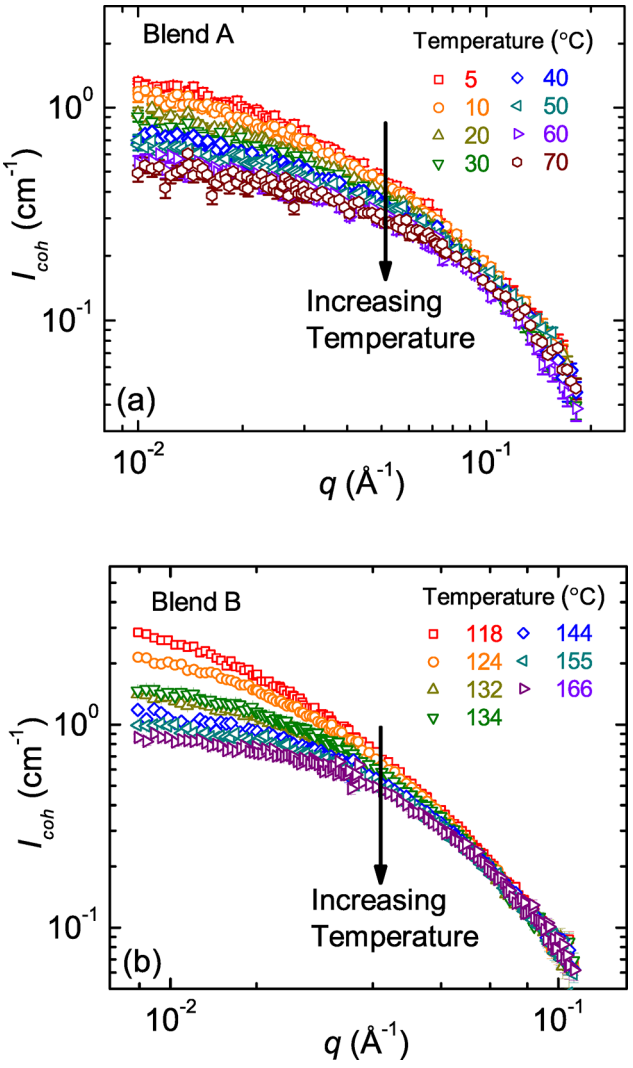

Figure 1. (a) Temperature dependence of coherent scattering intensity I_{coh} as a function of scattering vector q for (a) blend A and (b) blend B. The error bars represent the uncertainty in I_{coh}. In many cases, error bars are smaller than the data points and not shown. Data obtained on pure blend components are shown in Figures S7–S9.

where $S(q)$ is the q-dependent structure factor (related to the coherent scattering intensity through the contrast) and ϕ_1 is the volume fraction of component 1. The coherent scattering intensity is then given by

$$I_{coh}(q \to 0) = (B_1 - B_2)^2 S(q \to 0) = (B_1 - B_2)^2 v_{ref}\left(\frac{1}{N_1\phi_1} + \frac{1}{N_2\phi_2} - 2\chi\right)^{-1} \quad (3)$$

$$B_i = \frac{\sum_j b_j}{v_{mon,i}} \quad (4)$$

where N_i, ϕ_i, and B_i are the number of repeat units (based on a chosen reference volume v_{ref} of 100 Å^3), volume fraction, and scattering length density of component i (B_i is calculated by summing over the scattering lengths of each atom in the C_4 monomer repeat unit and dividing by the monomer repeat unit volume, $v_{mon,i}$). N_i is calculated as $N_i = N_{mon,i}v_{mon,i}/v_{ref}$, where $N_{mon,i}$ is the number of monomer repeat units. $v_{mon,i}$ is calculated using the measured polymer density and reported volumetric thermal expansion coefficient (0.000 68 K^{-1}).[48] χ is the Flory–Huggins interaction parameter and for the purposes of this analysis assumed to be independent of blend composition and molecular weight.

A Zimm plot, which shows $(I_{coh}(q))^{-1}$ as a function of q^2, is a convenient method to accurately characterize $I_{coh}(q \to 0)$. Linear behavior of $(I_{coh}(q))^{-1}$ as a function of q^2 is anticipated over q values wherein $qR_g \ll 1$. Figure 2 shows Zimm plots for blends A and B, in which the inverse of the intercept of a linear fit to the data provided quantification of $I_{coh}(q \to 0)$. This process was repeated for data taken at various temperatures, and each $I_{coh}(q \to 0)$ value was then used to extract χ using eq 3, in which all other parameters were independently characterized. The low temperature limit of SANS measurements was defined by the blend spinodal temperature (summarized in Table S1, obtained from plots of $1/I(0)$ vs T^{-1} shown in Figure S10). At temperatures well above the spinodal, the scattering intensity is insensitive to χ, thus limiting the range of temperatures over which χ can be characterized for a given blend. For this reason, two blends of differing molecular weight were explored (Table 1), allowing access to a wide temperature range for characterization of χ.

Additionally, we analyzed the full I_{coh} vs q scattering profiles with the random phase approximation (eq 5), which provides information on both χ and the chain dimensions of the components of polymer blends.

$$I_{coh}(q) = (B_1 - B_2)^2 v_{ref}\left(\frac{1}{N_1\phi_1 P_1(q)} + \frac{1}{N_2\phi_2 P_2(q)} - 2\chi\right)^{-1} \quad (5)$$

For Gaussian chains, the form factor $P_i(q)$ is described as

DOI: 10.1021/acs.macromol.7b02181
Macromolecules 2018, 51, 3107–3115

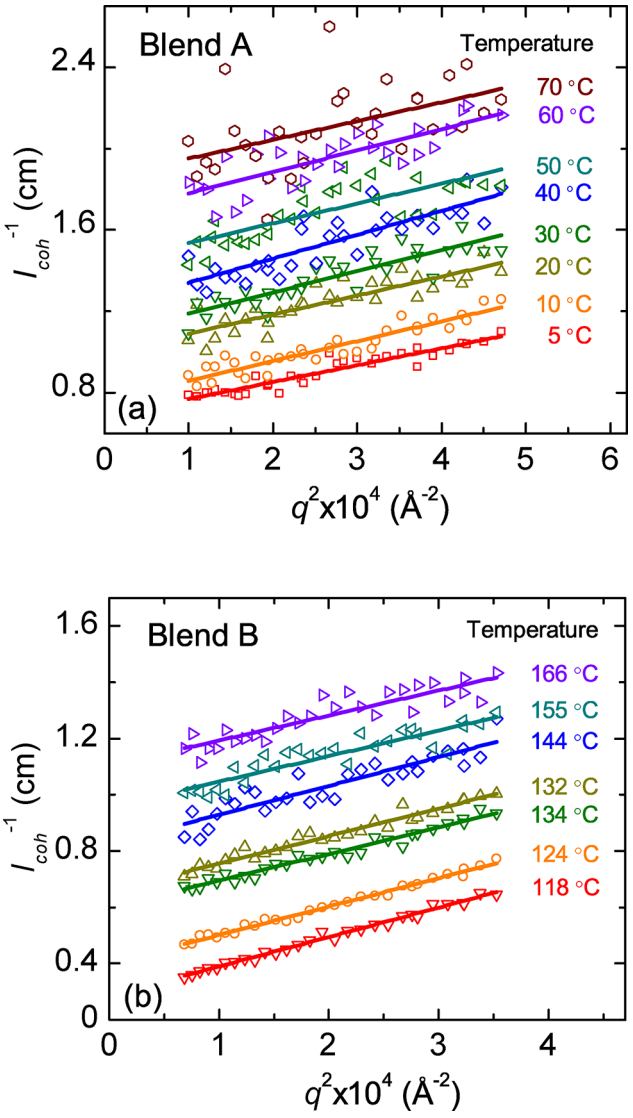

Figure 2. Zimm plot showing I_{coh}^{-1} vs q^2 for (a) blend A and (b) blend B. Solid lines represent linear fits to the data. χ is calculated from the value of I_{coh} at $q \rightarrow 0$, determined as 1/intercept of the Zimm plot.

$$P_i(q) = \frac{2}{x_i^2}(e^{-x_i} - 1 + x_i) \quad (6)$$

where $x_i = q^2R_{g,i}^2 = q^2N_il_i^2/6$; $R_{g,i}$, N_i, and l_i are the radius of gyration, number of repeat units, and statistical segment length of component i. A chain expansion factor, α, was applied which allowed for variations in the R_g values of the polymers due to the presence of the other blend component:

$$R_{g,i} = \alpha R_{g,i,theor} \quad (7)$$

where $R_{g,i,theor}$ is calculated based on literature values of l (l_{ref}) (6 and 5 Å for 1,2-polybutadiene[43] and saturated 1,2-polybutadiene,[50] respectively, based on a monomer C_4 repeat unit). Representative fits to the data are shown in Figure 3. The fitting parameters employed in the random phase approximation were χ and α. The blend components were assumed to undergo similar degrees of expansion in the blend, and therefore one value of α was applied to both (Tables S2 and S3). The temperature dependencies of the resulting R_g values of the blend components are shown in Figure 4. We note that the fitted values for R_g are significantly larger than those reported previously for the

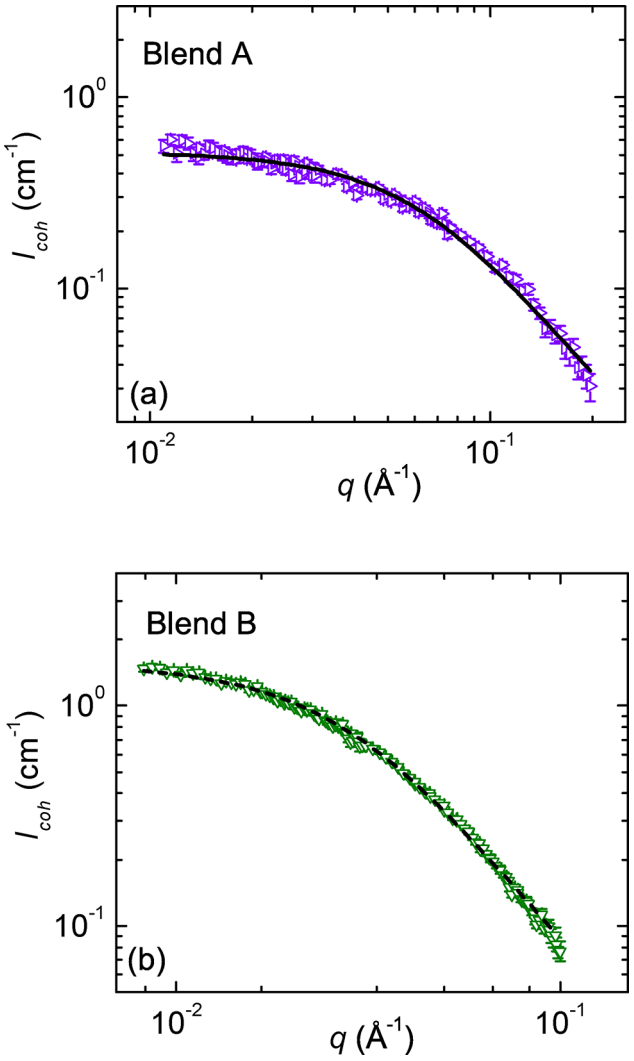

Figure 3. SANS data obtained from (a) blend A at 60 °C and (b) blend B at 134 °C. The random phase approximation (eq 5) was fit to the data. χ and α were adjustable parameters in the data fitting. The error bars represent the uncertainty in I_{coh}. In many cases, error bars are smaller than the data points and not shown. Fits to data obtained at other temperatures are shown in Figures S11 and S12, and Kratky plots are given in Figure S13.

unperturbed dimensions of significantly higher molecular weight polymers.[43,50] Taking the value of R_g determined from RPA fitting, we verified that the q range used for the Zimm analysis meets the condition of $qR_g \ll 1$. While the RPA analysis provided a reasonable fit to the data obtained from blend B, in the case of blend A the RPA fit underestimated the intensity at the low-q plateau, the region of the data at which the χ parameter is characterized, leading to greater discrepancy between Zimm and RPA analyses in the characterization of χ for blend A. The quality of fit was not improved through utilization of the wormlike chain model for the smaller molecular weight components in blend A (shown in Figure S14). The quality of fit may be impacted by the low molecular weights of the polymers, which leads to low coherent scattering intensity (and thus relatively large incoherent intensity), as well as data smearing (which was not accounted for in the model). We therefore emphasize the results of the Zimm analysis in quantifying the χ parameter obtained from blend A.

The behavior of χ as a function of inverse temperature, obtained through Zimm analysis of SANS data from blends A

DOI: 10.1021/acs.macromol.7b02181
Macromolecules 2018, 51, 3107−3115

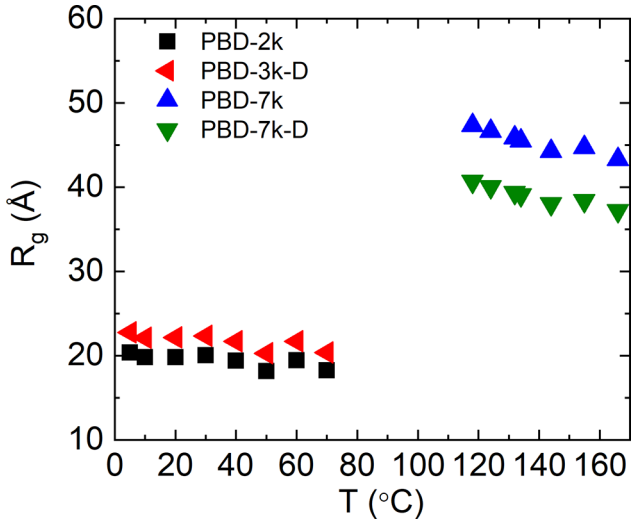

Figure 4. Temperature dependence of the radius of gyration, R_g, of components in blend A (PBD-2k and PBD-3k-D) and blend B (PBD-7k and PBD-7k-D). R_g values were calculated from the fit of the random phase approximation (eq 5) to the data.

and B as well as fitting the random phase approximation to data from blend B, is shown in Figure 5 (and tabulated in Tables S2–S5). A linear fit in the form of $\chi = A(T^{-1}) + B$ describes the data well, indicating that the small differences in 1,2 content of the components of the two blends, as well as molecular weight, have negligibly small impact on the values of χ. The agreement of $\chi(T^{-1})$ among these two blends of differing molecular weight indicates consistency with Flory–Huggins theory and suggests that at least for the current study, the thermodynamic properties are more mean-field-like than fluctuation-dominated.[51,52]

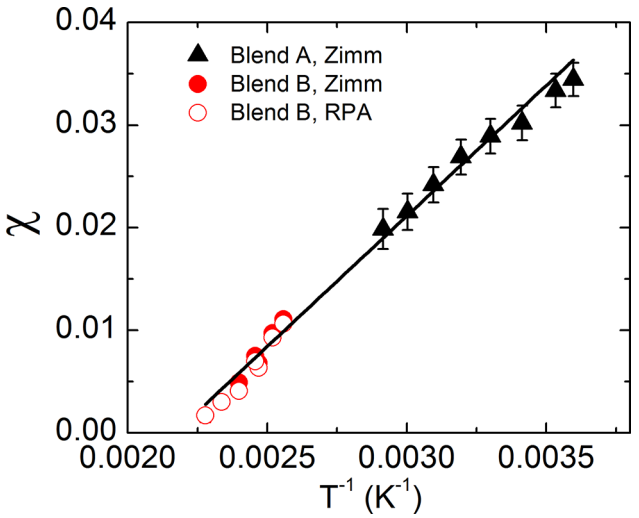

Figure 5. Flory–Huggins interaction parameter, χ, as a function of T^{-1}, obtained through Zimm analysis of SANS data for blends A and B, and fit of the random phase approximation (eq 5) to the SANS data obtained from blend B. χ is based on a reference volume of 100 Å^3. The solid curve represents a linear fit to the data (which accounts for the error in χ) of the form $\chi = A/T + B$, where $A = 25.5 \pm 0.8$ and $B = -0.055 \pm 0.002$. The R^2 value of the linear fit to the data was 0.985. The error bars represent the uncertainty in χ. In many cases, error bars are smaller than the data points and not shown. We also conducted linear fits to data obtained from blends A and B separately. For blend A, $A = 21.2 \pm 0.8$ and $B = -0.042 \pm 0.003$. For blend B, $A = 33.0 \pm 2.4$ and $B = -0.074 \pm 0.006$.

The errors on the quantified χ parameters were determined through analysis of the following sources: (1) error in molecular weight measurement, originating through uncertainty in the characterized dn/dc values and error in measured light scattering intensity, (2) error in density measurement, (3) error in the measured I_{coh}, most significant for the lower molecular weight blend A and for blend B at high temperatures, (4) error in extrapolation of data taken at finite q to $q \rightarrow 0$ (conducted through Zimm analysis), and (5) error in determination of the temperature-dependent incoherent scattering (obtained through a plot of $I_{total}q^4$ vs q^4, where I_{total} is the total scattering intensity including coherent and incoherent scattering, in the high q region, $q = 2-3$ nm^{-1}, in which the slope provided the incoherent scattering). These sources of error were propagated in the Zimm analysis used to quantify χ and are illustrated as error bars provided in Figure 5.

The measured $\chi(T^{-1})$ behavior of the 1,2-PBD/saturated 1,2-PBD blend was compared to literature values of χ for polydiene/polyolefin pairs, as shown in Figure 6. At low temperatures, χ of the 1,2-PBD system approaches that observed in a blend of polyisoprene (PI) and saturated PI of high 1,4-content.[34] χ of the 1,2-PBD system decreases more rapidly at high temperatures than that of the 1,4-PI system. At low temperatures, the χ parameters for both the 1,2-PBD and 1,4-PI systems are significantly higher than that measured for a blend of 1,4-PI and saturated 1,2-PBD.[35] All of the polydiene/polyolefin blends exhibit χ parameters which are larger in magnitude and have stronger temperature dependencies than that typically observed in polyolefin/polyolefin blends and polydiene/polydiene blends.[10]

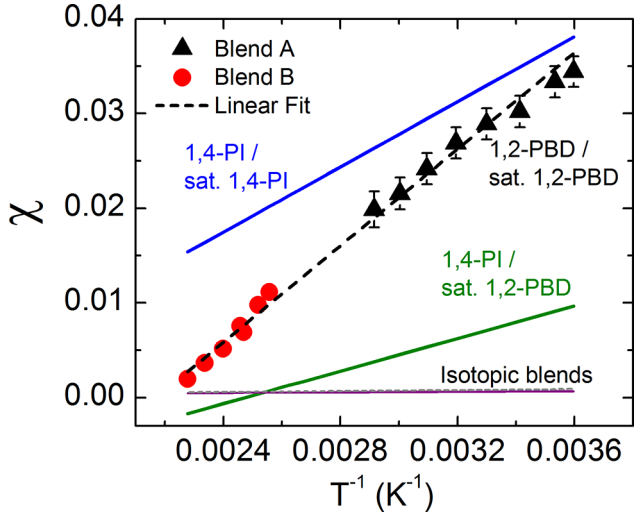

Figure 6. (a) Flory–Huggins interaction parameter, χ, as a function of T^{-1}, obtained through Zimm analysis for the 1,2-PBD/saturated 1,2-PBD blend [blend A (black ▲), blend B (red ●), linear fit to data (black dashed line)] compared to χ obtained from other polydiene/polyolefin systems: (1) PI/saturated (deuterated) PI with 93% 1,4-content (blue solid line)[34] and (2) PI (94% 1,4-content)/saturated PBD (99% 1,2-content) (green solid line).[35] Additionally, isotopic blends are shown of (1) the polydiene blend of 1,2-PBD/perdeuterated 1,2-PBD (97% 1,2-content, purple solid line) and (2) the polyolefin blend of fully hydrogenated and deuterated PBD (97% 1,2-content, gray dashed line).[43] χ is based on a reference volume of 100 Å^3. Linear fits of χ vs T^{-1} for reference data were obtained from ref 10.

Our data represent the first measurement of the χ parameter for 1,2-PBD/saturated 1,2-PBD. The interactions between the

DOI: 10.1021/acs.macromol.7b02181
Macromolecules 2018, 51, 3107–3115

polyolefin/polydiene pair are significant. We also note that there is negligible impact of characterizing the polymer interactions in blends which contain deuterated components: the isotopic effect is quite small, and the χ parameter reported for a blend of 1,2-PBD with perdeuterated 1,2-PBD (C_4H_4 and C_4D_4 repeat units, respectively) and that reported for a blend of hydrogenated 1,2-PBD and deuterated 1,2-PBD (both fully saturated) are significantly smaller than the interactions measured here for 1,2-PBD/saturated 1,2-PBD,[43] also shown in Figure 6.

Prediction of χ from Pressure−Volume−Temperature (*PVT*) Data. As noted by Graessley and co-workers,[53] *PVT* data and their fits to equations of state (such as the free volume idea embodied through the Flory−Orwoll−Vrij (FOV) equation of state that obeys the *corresponding states* principle) allow for an evaluation of thermodynamic interaction parameters for polymer blends. The FOV equation of state is written as

$$\frac{\tilde{P}\tilde{V}}{\tilde{T}} = \frac{\tilde{V}^{1/3}}{\tilde{V}^{1/3} - 1} - \frac{1}{\tilde{T}\tilde{V}} \tag{8}$$

where $P = P/P^*$, $T = T/T^*$, and $V = V/V^*$, with P^*, T^*, and V^* are the characteristic pressure, temperature, and volume, respectively. Yi and Zoller analyzed the *PVT* properties for a series of polydienes and fit the data to various equations of state; they provided values for the reduced parameters for various PBD and PI materials by fitting the data over 25−200 °C and 10−200 MPa.[54] Similarly, Walsh and co-workers reported the *PVT* properties of various polyolefins by fitting data between 150 and 250 °C and 10 to 200 MPa.[55,56] Further, using the Tait equation coefficients provided by Yi and Zoller, the solubility parameter (δ_{PVT}) of polymers were also deduced.[53] The tabulated values, as reduced by Graessley, are presented in Table 2.[53,55]

Interaction parameters were estimated using two key contributions: (a) the interaction strength X_{CED}, resulting from differences in cohesive energy density, calculated as $X_{CED} = (\delta_1 - \delta_2)^2$ (where δ_1 and δ_2 are the solubility parameters of the blend components) and (b) the free volume contribution X_{FV}, reflecting differences in component free volumes and captured through differences in T^* or through differences in α. X_{FV} is given mathematically by Graessley to be

$$X_{FV}\ (\text{MPa}) = 46\frac{(T_1^* - T_2^*)^2}{(\bar{T}^*)^2} \tag{9}$$

$$X_{FV}\ (\text{MPa}) = 14\frac{(\alpha_1^* - \alpha_2^*)^2}{(\bar{\alpha}^*)^2} \tag{10}$$

We estimate a thermodynamic interaction parameter for each blend pair (Table 3) using

$$\chi = \frac{V_{ref}}{RT}(X_{CED} + X_{FV}) \tag{11}$$

where V_{ref} is the reference volume in units of volume/mol.

The predicted value of χ at 167 °C for the 1,2-PBD/sat. 1,2-PBD blend is 2.2×10^{-3}, which is close to that measured experimentally (2.9×10^{-3}, as determined from the linear fit in Figure 5). There are, however, limitations to this approach. Graessley notes that there are two major concerns with the use of *PVT* data toward the estimation of thermodynamic interactions. First, there are systematic differences between experimental data and the FOV equation of state especially when compared to other EOS models. Moreover, the values of P^* and T^* obtained from the fits of the experimental data to the FOV model vary with the ranges of P and T covered in the fitting. Second, the accuracy and precision of the *PVT* data is somewhat questionable because of the relatively incompressible nature of polymers and the dependence of thermodynamic interactions to scale as differences of P^* and T^*. Nevertheless, as observed from the data presented above, the *PVT*-based estimate provides a reasonable quantification of χ for the case of the 1,2-PBD/saturated 1,2-PBD blend at high temperatures. We note that the *PVT* data do not provide any basis to anticipate the strong temperature dependence for χ that we observe. We further note that it would be interesting to compare the predictions of Lipson's recent modeling of *PVT* data with the data reported in this work.[57,58]

Table 2. Reduction Parameters from *PVT* Data Fit to Flory−Orwoll−Vrij Equation of State[a]

polymer	P^*	T^*	V^*	δ_{PVT} ($MPa^{1/2}$) at 167 °C	α (K^{-1}) × 10^4
PBD-8[b]	508	6827	0.9518	18.18	7.24
PBD-24	480	6873	0.9571	17.91	7.19
PBD-40	456	6914	0.9545	17.50	6.94
PBD-50	424	6994	0.9567	17.33	6.99
PBD-87	395	7040	0.9653	16.40	6.66
PBD-100 (extrapolated)[c]	368	7093		16.14	6.57
PI-8[a]	417	7032	0.9604	17.03	6.69
saturated 1,2-PBD (e.g., poly(1-butene))	409	7043	0.9832	15.86	7.01
saturated 1,4-PI (e.g., PEP)	458	6888	1.0031	16.74	7.33
polyethylene	490	6827	1.0047	17.67	7.80
polypropylene	403	6738	0.9983	15.87	7.52

[a]Values in table obtained from ref 53. [b]PBD-*X* is polybutadiene with *X* % 1,2-content, PI-8 is polyisoprene with 92% 1,4-content. [c]Linear extrapolation from the series of mixed microstructure polybutadiene samples.

Table 3. Estimates of Cohesive Energy Density and Free Volume Contributions to the Thermodynamic Interaction Parameters for Blends of Polyolefins and Polydienes at 167 °C

blend components[a]	X_{CED}	$X_{FV}(T^*)$	$X_{FV}(\alpha)$	$X = X_{CED} + X_{FV}(T^*)$	$\chi = (V_{ref} X)/RT$
PBD-100/sat. PBD-100	0.08	0.00_2	0.06	0.08_2	2.2×10^{-3}
PI-8/PEP	0.08	0.02	0.11	0.10	2.7×10^{-3}
PBD-100/PP	0.07	0.12	0.25	0.19	5.2×10^{-3}
PBD-100/PEP	0.36	0.04	0.17	0.40	10.9×10^{-3}
PBD-100/PE	2.34	0.07	0.41	2.41	65.9×10^{-3}
PI-8/sat. PBD-100	1.37	0.00	0.03	1.37	37.5×10^{-3}
PI-8/PP	1.35	0.08	0.19	1.43	39.1×10^{-3}
PI-8/PE	0.41	0.04	0.33	0.45	12.3×10^{-3}

[a]PBD-*X* is polybutadiene with *X*% 1,2-content, PI-8 is polyisoprene with 92% 1,4-content, PEP is saturated 1,4-PI, PP is polypropylene, and PE is polyethylene. All χ parameters calculated based on a reference volume of 100 Å^3.

CONCLUSIONS

The Flory−Huggins interaction parameter, χ, of a blend of 1,2-polybutadiene (1,2-PBD)/saturated 1,2-PBD has been characterized through small-angle neutron scattering (SANS). SANS data obtained from single phase blends were analyzed through Zimm analysis and fitting of the random phase approximation.

DOI: 10.1021/acs.macromol.7b02181
Macromolecules 2018, 51, 3107−3115

The temperature dependencies of χ extracted by the two methods were in good agreement. The resulting χ parameter was large and strongly temperature-dependent, in stark contrast to behavior previously reported for more commonly studied polyolefin pairs and polydiene pairs. The χ parameter of 1,2-PBD/saturated 1,2-PBD approached that previously reported for a blend of 1,4-polyisoprene (1,4-PI) and saturated 1,4-PI. The 1,2-PBD system exhibited a stronger temperature dependence of χ as compared to the 1,4-PI system. At low temperatures, the χ parameters for both the 1,2-PBD and 1,4-PI systems were significantly higher than that previously reported for a blend of 1,4-PI and saturated 1,2-PBD. The measured χ of 1,2-PBD/saturated 1,2-PBD, at high temperatures, was in good agreement with solubility parameter predictions based on *PVT* properties of the individual components.

■ ASSOCIATED CONTENT

Supporting Information

The Supporting Information is available free of charge on the ACS Publications website at DOI: 10.1021/acs.macromol.7b02181.

$I_{total}q^4$ vs q^4 (Figure S1); ^{1}H NMR data obtained from DIPIP (Figure S2) and components of blends A and B (Figures S3, S4); GPC data obtained from blend components (Figure S5); I_{total} vs q (Figure S6); I_{total} and I_{coh} obtained from blend components (Figures S7−S9); $1/I(0)$ vs T^{-1} from blends (Figure S10) and resulting spinodal temperatures (Table S1); RPA fitting to I_{coh} vs q for blends A and B at various temperatures (Figures S11, S12); Kratky plots (Figure S13); RPA fitting to I_{coh} vs q for blend A at various temperatures using the wormlike chain model (Figure S14); and χ and α extracted from data analysis (Tables S2−S5) (PDF)

■ AUTHOR INFORMATION

Corresponding Authors

*(R.K.) E-mail ramanan@uh.edu; Tel 713-743-4307.
*(M.L.R.) E-mail mlrobertson@uh.edu; Tel 713-743-2748.

ORCID

Ruixuan Han: 0000-0001-7867-3043
Carlos R. López-Barrón: 0000-0002-9620-0298
Megan L. Robertson: 0000-0002-2903-3733
Ramanan Krishnamoorti: 0000-0001-5831-502X

Author Contributions

J.Q. and K.I.M. contributed equally to this work.

Notes

The authors declare no competing financial interest.

■ ACKNOWLEDGMENTS

We thank Ryan Poling-Skutvik for helpful discussions on SANS data analysis. Access to NG-7 and NGB was provided by the Center for High Resolution Neutron Scattering, a partnership between the National Institute of Standards and Technology and the National Science Foundation under Agreement No. DMR-1508249. We acknowledge the support of National Institute of Standards and Technology, U.S. Department of Commerce, in providing the neutron research facilities used in this work. We gratefully acknowledge the contributions of Yun Liu and Yimin Mao for assistance with SANS data acquisition and analysis. This work is supported by ExxonMobil Chemical Company.

■ REFERENCES

(1) Helfand, E.; Tagami, Y. Theory of the interface between immiscible polymers. II. *J. Chem. Phys.* **1972**, *56* (7), 3592−3601.
(2) Chaturvedi, U. K.; Steiner, U.; Zak, O.; Krausch, G.; Klein, J. Interfacial structure in polymer mixtures below the critical point. *Phys. Rev. Lett.* **1989**, *63* (6), 616.
(3) Zhang, W.; Gomez, E. D.; Milner, S. T. Predicting Flory-Huggins χ from Simulations. *Phys. Rev. Lett.* **2017**, *119* (1), 017801.
(4) Bartczak, Z.; Galeski, A. Mechanical Properties of Polymer Blends. In *Polymer Blends Handbook*; Utracki, L. A., Wilkie, C. A., Eds.; Springer Netherlands: Dordrecht, 2014; pp 1203−1297.
(5) Matsen, M. W.; Bates, F. S. Unifying weak- and strong-segregation block copolymer theories. *Macromolecules* **1996**, *29* (4), 1091−1098.
(6) Park, C.; Yoon, J.; Thomas, E. L. Enabling nanotechnology with self assembled block copolymer patterns. *Polymer* **2003**, *44* (22), 6725−6760.
(7) Flory, P. J. Thermodynamics of high polymer solutions. *J. Chem. Phys.* **1942**, *10*, 51−61.
(8) Huggins, M. L. Some properties of solutions of long-chain compounds. *J. Chem. Phys.* **1942**, *46*, 151−158.
(9) Matsen, M. W. The standard Gaussian model for block copolymer melts. *J. Phys.: Condens. Matter* **2002**, *14* (2), R21−R47.
(10) Eitouni, H. B.; Balsara, N. P. Thermodynamics of Polymer Blends. In *Physical Properties of Polymers Handbook*, 2nd ed.; Mark, J. E., Ed.; Springer: New York, 2007.
(11) Sakurai, S.; Hasegawa, H.; Hashimoto, T.; Hargis, I. G.; Aggarwal, S.; Han, C. C. Microstructure and isotopic labeling effects on the miscibility of polybutadiene blends studied by the small-angle neutron scattering technique. *Macromolecules* **1990**, *23* (2), 451−459.
(12) Bates, F. S.; Hartney, M. A. Block copolymers near the microphase separation transition. 3. Small-angle neutron scattering study of the homogeneous melt state. *Macromolecules* **1985**, *18* (12), 2478−2486.
(13) Hasegawa, H.; Sakurai, S.; Takenaka, M.; Hashimoto, T.; Han, C. C. Small-angle neutron scattering and light scattering studies on the miscibility of protonated polyisoprene/deuterated polybutadiene blends. *Macromolecules* **1991**, *24* (8), 1813−1819.
(14) Tomlin, D.; Roland, C. Negative excess enthalpy in a van der Waals polymer mixture. *Macromolecules* **1992**, *25* (11), 2994−2996.
(15) Graessley, W.; Krishnamoorti, R.; Balsara, N.; Butera, R.; Fetters, L.; Lohse, D.; Schulz, D.; Sissano, J. Thermodynamics of mixing for blends of model ethylene-butene copolymers. *Macromolecules* **1994**, *27* (14), 3896−3901.
(16) Balsara, N.; Fetters, L.; Hadjichristidis, N.; Lohse, D.; Han, C.; Graessley, W.; Krishnamoorti, R. Thermodynamic interactions in model polyolefin blends obtained by small-angle neutron scattering. *Macromolecules* **1992**, *25* (23), 6137−6147.
(17) Krishnamoorti, R.; Graessley, W. W.; Balsara, N. P.; Lohse, D. J. The compositional dependence of thermodynamic interactions in blends of model polyolefins. *J. Chem. Phys.* **1994**, *100* (5), 3894−3904.
(18) Krishnamoorti, R.; Graessley, W. W.; Balsara, N. P.; Lohse, D. J. Structural origin of thermodynamic interactions in blends of saturated hydrocarbon polymers. *Macromolecules* **1994**, *27* (11), 3073−3081.
(19) Rosedale, J. H.; Bates, F. S.; Almdal, K.; Mortensen, K.; Wignall, G. D. Order and disorder in symmetric diblock copolymer melts. *Macromolecules* **1995**, *28* (5), 1429−1443.
(20) Graessley, W. W.; Krishnamoorti, R.; Reichart, G. C.; Balsara, N. P.; Fetters, L. J.; Lohse, D. J. Regular and irregular mixing in blends of saturated hydrocarbon polymers. *Macromolecules* **1995**, *28* (4), 1260−1270.
(21) Reichart, G. C.; Graessley, W. W.; Register, R. A.; Krishnamoorti, R.; Lohse, D. J. Anomalous Attractive Interactions in Polypropylene Blends. *Macromolecules* **1997**, *30* (10), 3036−3041.
(22) Wachowicz, M.; Gill, L.; Wolak, J.; White, J. L. Polypropylene and Polyethylene−Copolymer Blend Miscibility: Slow Chain Dynamics in Individual Blend Components near the Glass Transition. *Macromolecules* **2008**, *41* (8), 2832−2838.
(23) Xu, J.; Mittal, V.; Bates, F. S. Toughened Isotactic Polypropylene: Phase Behavior and Mechanical Properties of Blends with Strategically

DOI: 10.1021/acs.macromol.7b02181
Macromolecules 2018, 51, 3107−3115

Designed Random Copolymer Modifiers. *Macromolecules* **2016**, *49* (17), 6497−6506.
(24) Beckingham, B. S.; Burns, A. B.; Register, R. A. Mixing Thermodynamics of Ternary Block−Random Copolymers Containing a Polyethylene Block. *Macromolecules* **2013**, *46* (7), 2760−2766.
(25) Chen, X.; Wignall, G. D.; He, L.; Lopez-Barron, C.; Alamo, R. G. SANS Evidence of Liquid−Liquid Phase Separation Leading to Inversion of Crystallization Rate of Broadly Distributed Random Ethylene Copolymers. *Macromolecules* **2017**, *50* (11), 4406−4414.
(26) Shin, T. J.; Lee, B.; Lee, J.; Jin, S.; Sung, B. S.; Han, Y. S.; Lee, C.-H.; Stein, R. S.; Ree, M. Small-angle neutron scattering study of the miscibility of metallocene-catalyzed octene linear low-density polyethylene and low-density polyethylene blends. *J. Appl. Crystallogr.* **2009**, *42* (2), 161−168.
(27) Zhang, X.; Man, X.; Han, C. C.; Yan, D. Nucleation induced by phase separation in the interface of polyolefin blend. *Polymer* **2008**, *49* (9), 2368−2372.
(28) Shin, K.; Nam, B. U.; Bang, J.; Jho, J. Y. Melt-state miscibility of poly(ethylene-co-1-octene) and linear polyethylene. *J. Appl. Polym. Sci.* **2008**, *107* (4), 2584−2587.
(29) Alamo, R.; Londono, J.; Mandelkern, L.; Stehling, F.; Wignall, G. Phase behavior of blends of linear and branched polyethylenes in the molten and solid states by small-angle neutron scattering. *Macromolecules* **1994**, *27* (2), 411−417.
(30) Nedoma, A. J.; Robertson, M. L.; Wanakule, N. S.; Balsara, N. P. Measurements of the Composition and Molecular Weight Dependence of the Flory−Huggins Interaction Parameter. *Macromolecules* **2008**, *41* (15), 5773−5779.
(31) Chen, Q. P.; Chu, J. D.; DeJaco, R. F.; Lodge, T. P.; Siepmann, J. I. Molecular Simulation of Olefin Oligomer Blend Phase Behavior. *Macromolecules* **2016**, *49* (10), 3975−3985.
(32) Krishnamoorti, R.; Graessley, W. W.; Fetters, L. J.; Garner, R. T.; Lohse, D. J. Anomalous mixing behavior of polyisobutylene with other polyolefins. *Macromolecules* **1995**, *28* (4), 1252−1259.
(33) Reynolds, B. J.; Ruegg, M. L.; Balsara, N. P.; Radke, C. J.; Shaffer, T. D.; Lin, M. Y.; Shull, K. R.; Lohse, D. J. Thermodynamics of polymer blends organized by balanced block copolymer surfactants studied by mean-field theories and scattering. *Macromolecules* **2004**, *37* (19), 7401−7417.
(34) Bates, F. S.; Rosedale, J. H.; Stepanek, P.; Lodge, T. P.; Wiltzius, P.; Fredrickson, G. H.; Hjelm, R. P. Static and dynamic crossover in a critical polymer mixture. *Phys. Rev. Lett.* **1990**, *65* (15), 1893−1896.
(35) Davidock, D. A.; Hillmyer, M. A.; Lodge, T. P. Mapping Large Regions of Diblock Copolymer Phase Space by Selective Chemical Modification. *Macromolecules* **2004**, *37* (2), 397−407.
(36) Zhao, Y.; Cai, S.; Li, J.; Wang, D. Z. Visible-light photo-catalytic C−C bond cleavages: preparations of N,N-dialkylformamides from 1,2-vicinal diamines. *Tetrahedron* **2013**, *69* (38), 8129−8131.
(37) Bartell, L. S.; Roskos, R. R. Isotope Effects on Molar Volume and Surface Tension: Simple Theoretical Model and Experimental Data for Hydrocarbons. *J. Chem. Phys.* **1966**, *44* (2), 457−463.
(38) Bates, F. Small-angle neutron scattering from amorphous polymers. *J. Appl. Crystallogr.* **1988**, *21* (6), 681−691.
(39) Bates, F.; Keith, H.; McWhan, D. Isotope effect on the melting temperature of nonpolar polymers. *Macromolecules* **1987**, *20* (12), 3065−3070.
(40) Glinka, C.; Barker, J.; Hammouda, B.; Krueger, S.; Moyer, J.; Orts, W. The 30 m small-angle neutron scattering instruments at the National Institute of Standards and Technology. *J. Appl. Crystallogr.* **1998**, *31* (3), 430−445.
(41) Kline, S. SANS data reduction tutorial. NIST Center for Neutron Research, 2001.
(42) Balsara, N.; Lohse, D.; Graessley, W.; Krishnamoorti, R. Small-angle neutron scattering by partially deuterated polymers and their blends. *J. Chem. Phys.* **1994**, *100* (5), 3905−3910.
(43) Bates, F. S.; Fetters, L. J.; Wignall, G. D. Thermodynamics of isotopic polymer mixtures: poly(vinylethylene) and poly-(ethylethylene). *Macromolecules* **1988**, *21* (4), 1086−1094.
(44) Halasa, A. F.; Lohr, D. F.; Hall, J. E. Anionic polymerization to high vinyl polybutadiene. *J. Polym. Sci., Polym. Chem. Ed.* **1981**, *19* (6), 1357−1360.
(45) Han, C. D.; Chun, S. B.; Hahn, S. F.; Harper, S. Q.; Savickas, P. J.; Meunier, D. M.; Li, L.; Yalcin, T. Phase Behavior of Polystyrene/Polybutadiene and Polystyrene/Hydrogenated Polybutadiene Mixtures: Effect of the Microstructure of Polybutadiene. *Macromolecules* **1998**, *31* (2), 394−402.
(46) Xu, Z.; Hadjichristidis, N.; Carella, J. M.; Fetters, L. J. Characteristic ratios of atactic poly(vinylethylene) and poly-(ethylethylene). *Macromolecules* **1983**, *16* (6), 925−929.
(47) Fetters, L. J. Procedures for homogeneous anionic polymerization. *J. Res. Natl. Bur. Stand., Sect. A* **1966**, *70A* (6), 421−433.
(48) Roovers, J.; Toporowski, P. Microheterogeneity in miscible blends of 1, 2-polybutadiene and 1, 4-polyisoprene. *Macromolecules* **1992**, *25* (13), 3454−3461.
(49) Krishnamoorti, R. PhD Thesis, Princeton University, 1994.
(50) Bates, F. S.; Schulz, M. F.; Rosedale, J. H.; Almdal, K. Correlation of binary polyolefin phase behavior with statistical segment length asymmetry. *Macromolecules* **1992**, *25* (20), 5547−5550.
(51) Beardsley, T. M.; Matsen, M. W. Fluctuation correction for the critical transition of symmetric homopolymer blends. *J. Chem. Phys.* **2017**, *147* (4), 044905.
(52) Gillard, T. M.; Medapuram, P.; Morse, D. C.; Bates, F. S. Fluctuations, Phase Transitions, and Latent Heat in Short Diblock Copolymers: Comparison of Experiment, Simulation, and Theory. *Macromolecules* **2015**, *48* (8), 2801−2811.
(53) Graessley, W. W. *Polymeric Liquids & Networks: Structure and Properties*; Garland Science (Taylor & Francis Group): New York, 2004.
(54) Yi, Y. X.; Zoller, P. An experimental and theoretical study of the PVT equation of state of butadiene and isoprene elastomers to 200°C and 200 MPa. *J. Polym. Sci., Part B: Polym. Phys.* **1993**, *31* (7), 779−788.
(55) Krishnamoorti, R.; Graessley, W. W.; Dee, G. T.; Walsh, D. J.; Fetters, L. J.; Lohse, D. J. Pure Component Properties and Mixing Behavior in Polyolefin Blends. *Macromolecules* **1996**, *29* (1), 367−376.
(56) Walsh, D.; Graessley, W.; Datta, S.; Lohse, D.; Fetters, L. Equations of state and predictions of miscibility for hydrocarbon polymers. *Macromolecules* **1992**, *25* (20), 5236−5240.
(57) White, R. P.; Lipson, J. E. G. Free Volume, Cohesive Energy Density, and Internal Pressure as Predictors of Polymer Miscibility. *Macromolecules* **2014**, *47* (12), 3959−3968.
(58) White, R. P.; Lipson, J. E. G.; Higgins, J. S. New Correlations in Polymer Blend Miscibility. *Macromolecules* **2012**, *45* (2), 1076−1084.

DOI: 10.1021/acs.macromol.7b02181
Macromolecules 2018, 51, 3107−3115